Development 135, 1693-1702 (2008) doi:10.1242/dev.016576

Tbx2b is required for the development of the parapineal organ

Corey D. Snelson[1], Kirankumar Santhakumar[2], Marnie E. Halpern[2] and Joshua T. Gamse[1,*]

Structural differences between the left and right sides of the brain exist throughout the vertebrate lineage. By studying the zebrafish pineal complex, which exhibits notable asymmetries, both the genes and the cell movements that result in left-right differences can be characterized. The pineal complex consists of the midline pineal organ and the left-sided parapineal organ. The parapineal is responsible for instructing the asymmetric architecture of the bilateral habenulae, the brain nuclei that flank the pineal complex. Using in vivo time-lapse confocal microscopy, we find that the cells that form the parapineal organ migrate as a cluster of cells from the pineal complex anlage to the left side of the brain. In a screen for mutations that disrupted brain laterality, we identified a nonsense mutation in the *T-box2b* (*tbx2b*) gene, which encodes a transcription factor expressed in the pineal complex anlage. The *tbx2b* mutant makes fewer parapineal cells, and they remain as individuals near the midline rather than migrating leftward as a group. The reduced number and incorrect placement of parapineal cells result in symmetric development of the adjacent habenular nuclei. We conclude that *tbx2b* functions to specify the correct number of parapineal cells and to regulate their asymmetric migration.

KEY WORDS: Left-right asymmetry, Pineal complex, Diencephalon, Epithalamus, Zebrafish, *from beyond* mutant

INTRODUCTION

The formation of an organ requires specification of multiple cell types within a primordium, followed by appropriate morphogenetic movements that shape the mature organ. In the case of asymmetrically shaped and positioned organs, morphogenesis must also be regulated along the left-right (L-R) axis. The zebrafish presents a unique opportunity to study the formation of an asymmetric region in the brain, namely the pineal complex, which is found in the dorsal diencephalon (epithalamus). The pineal complex includes the melatonin-secreting pineal organ and the left-sided parapineal organ (Butler and Hodos, 1996; Borg et al., 1983). In adult fish, the pineal organ is attached to the brain via a stalk, which emerges just to the left of the midline (Liang et al., 2000). The parapineal organ is situated within the brain to the left of the pineal stalk (Gamse et al., 2002). Adjacent to the pineal complex are the bilateral habenular nuclei (habenulae). Along with the medial forebrain bundle, the habenulae and their efferent connections are a principal pathway connecting the limbic forebrain with the midbrain. Habenular axons travel via the fasciculi retroflexus (FR) to the interpeduncular nucleus (IPN) of the midbrain; this habenulo-interpeduncular connection is highly conserved throughout the vertebrate lineage (Sutherland, 1982). In teleosts, including zebrafish, axons from the left versus right habenula innervate different dorsoventral regions of the IPN, in contrast to other vertebrates, in which the two habenulae exhibit similar connections to the IPN (Kuan et al., 2007a).

In zebrafish, the asymmetric location of the parapineal organ imposes laterality on the flanking habenulae, which exhibit L-R differences in their neuropil density (Concha et al., 2000) and in the size and expression of genes such as *leftover* (*lov*; also known as *kctd12.1* – ZFIN) (Gamse et al., 2003). In mutants in which the parapineal is on the right side of the brain, structural and gene expression differences in the habenulae are also L-R reversed (Gamse et al., 2003; Concha et al., 2000). Selective destruction of the parapineal by laser ablation reveals its instructive role on the left habenula. In the absence of the parapineal, both habenulae develop with equivalent size, patterns of gene expression, and neuropil density characteristic of the right habenula (Gamse et al., 2003; Concha et al., 2003). This abnormal development of the habenulae also affects efferent projections to the IPN. In wild-type (WT) embryos, the left habenular neurons project to both the dorsal and ventral regions of the IPN (Gamse et al., 2005; Aizawa et al., 2005). However, in parapineal-ablated larvae, left habenular neurons no longer project dorsally, but instead innervate the ventral IPN, characteristic of right habenular neurons (Gamse et al., 2005). Therefore, the development of the parapineal is important for asymmetry of the dorsal diencephalon as well as for the formation of diencephalic connectivity to other brain regions.

The parapineal organ is morphologically distinguishable between 28 and 32 hours post-fertilization (hpf) as a cluster of cells adjacent to the anterior left edge of the pineal anlage (Gamse et al., 2003; Concha et al., 2003). Studies of fixed samples suggest that over the course of the next 3 days, the parapineal becomes located more posteriorly and ventrally relative to the pineal organ (Gamse et al., 2002). A single parapineal organ is detected in 95% of WT zebrafish larvae on the left side of the brain, and only very rarely (<0.3%) are bilateral or no parapineal organs observed (Gamse et al., 2003; Concha et al., 2000). Precursors of the parapineal and pineal organ are thought to derive from a common pool of cells, as shown by lineage labeling of the pineal complex anlage at 22-24 hpf (Concha et al., 2003). The genes that regulate how parapineal cells are specified from this precursor pool, and that are responsible for their ultimate left-sided localization, are unknown.

To identify genes involved in asymmetric development of the epithalamus, we performed a genetic screen for mutations that disrupt L-R differences of *lov* expression in the habenulae. Here, we report the isolation and characterization of the *from beyond* (*fby*)

[1]Department of Biological Sciences, Vanderbilt University, VU Station B, Box 35-1634, Nashville, TN 37235, USA. [2]Department of Embryology, Carnegie Institution of Washington, 3520 San Martin Drive, Baltimore, MD 21218, USA.

*Author for correspondence (e-mail: josh.gamse@vanderbilt.edu)

Accepted 10 March 2008

mutation that produces homozygous embryos with reduced *lov* expression in the left habenula. We identify *fby* as a lesion in the *T-box2b* (*tbx2b*) gene that disrupts parapineal development. Time-lapse analysis reveals details of the morphogenetic process, showing that parapineal cells migrate leftward away from the pineal complex anlage as a cluster. By contrast, the parapineal cells of *fby* mutants are fewer in number and are scattered near the midline of the brain. We propose that Tbx2b assigns cells to the parapineal lineage and regulates their asymmetric migration.

MATERIALS AND METHODS

Zebrafish

Zebrafish were raised at 28.5°C on a 14/10 hour light/dark cycle and staged according to hpf or days post-fertilization (dpf). The wild-type strains AB (Walker, 1999) and WIK (Rauch et al., 1997), the transgenic lines Tg(*foxd3:*GFP)^{fkg17} and Tg(*foxd3:*GFP)^{fkg3} (Gilmour et al., 2002), the ethylnitrosourea-induced mutations *knypek*^{m119} and *trilobite*^{m747} (Solnica-Krezel et al., 1996), and *fby*^{c144} were used.

Mutagenesis and screening

ENU mutagenesis was performed by placing male zebrafish in 3 mM ENU for three 1-hour treatments with 48 hours between treatments. F1 fish were generated by crossing ENU-mutagenized males to AB females. F2 fish were generated by intercrossing F1 males and females. F3 larvae were generated from F2 intercrosses and at 4 dpf were fixed for in situ hybridization with the *lov* probe. Putative mutations showing reversed or bilaterally symmetric expression of *lov* in the habenular nuclei were re-identified in F2 heterozygotes and lines established through outcrosses to AB fish.

Cloning of *fby*

Heterozygous fish (AB background) carrying the *fby*^{c144} mutation were crossed with wild-type WIK fish. F2 mutant larvae were used for meiotic mapping with simple sequence length polymorphism (SSLP) markers, as previously described (Bahary et al., 2004). For identification of the lesion in the *tbx2b* gene, cDNA was prepared using Superscript II reverse transcriptase (Invitrogen) from mRNA isolated from 4-day-old AB and *fby* mutant larvae using Trizol (Invitrogen). For sequencing, cDNA was amplified using primers that flanked the *tbx2b* open reading frame and Pfu DNA polymerase, and subcloned into the pCRII-Topo vector (Invitrogen). Clones were sequenced using an ABI 3730xl sequencer and sequence data were analyzed with Sequencher software (GeneTools).

Genotyping *fby* mutants

To genotype larvae, DNA was extracted by boiling larvae for 10 minutes in 25 μl of Embryo Lysis Buffer (Bahary et al., 2004). Proteinase K (Roche Applied Bioscience) was added to a final concentration of 0.5 mg/ml and samples were incubated at 55°C for 2 hours, then boiled for 10 minutes to deactivate the proteinase K. The *fby* mutation introduces an *Mse*I restriction site at bp 134 of exon 3. Primers flanking this site were used to amplify genomic DNA (forward primer, 5′-TGTGACGAGCACTAATGTC-TTCCTC-3′; reverse primer, 5′-GCAAAAAGCATCGCAGAACG-3′). The PCR product was digested with *Mse*I (NEB) at 37°C for 1 hour, then run on a 3% agarose gel.

Morpholino injections

Antisense morpholino (MO) sequences for *tbx2b* were derived from the translation initiation site and the splice donor site of the third exon as described [Tbx2b-ATG and Tbx2b-SP (Gross and Dowling, 2005)]. The MO stock solution (10 mg/ml) was diluted to 6 ng/nl in distilled H_2O, and embryos (1- to 2-cell stage) were pressure-injected with ~1 nl to deliver 6 ng of MO per embryo. Embryos from the transgenic line Tg(*foxd3:*GFP)^{fkg17} were used so that the location of the parapineal could be readily assessed by fluorescence in live larvae at 3-4 dpf.

RNA in situ hybridization

Whole-mount RNA in situ hybridization was performed as described previously (Gamse et al., 2003), using reagents from Roche Applied Bioscience. RNA probes were labeled using fluorescein-UTP or digoxygenin-UTP. To synthesize antisense RNA probes, pBS-*otx5* (Gamse et al., 2002), *znot* (*flh*) (Talbot et al., 1995), pBS II SK-*znr1* (*cyc*) (Sampath et al., 1998), and pBK-CMV-*leftover* (Gamse et al., 2003) were linearized with *Eco*RI and transcribed with T7 RNA polymerase; pCRII-*tbx2b*, *zPitx2* (Tsukui et al., 1999) and pBK-CMV-*right on* (Gamse et al., 2005) with *Bam*HI and T7 RNA polymerase; pCRII-*dexter* (Gamse et al., 2005) with *Xho*I and SP6 RNA polymerase; pBS II SK–*ATV* (*lft1*) (Thisse and Thisse, 1999) with *Not*I and T7 RNA polymerase; pBSK+ *southpaw* (Long et al., 2003) with *Spe*I and T7 polymerase; pGEM-*fzd7a* (El-Messaoudi and Renucci, 2001) with *Apa*I and SP6 polymerase; pBS II SK-*wnt11* (Makita et al., 1998) with *Hin*dIII and T3 polymerase; and pBS-*gfi1* (Dufourcq et al., 2004) with *Sac*II and T3 RNA polymerase. Embryos were incubated at 70°C with probe and hybridization solution containing 50% formamide (60% for *cyc*). Hybridized probes were detected using alkaline phosphatase-conjugated antibodies and visualized by 4-nitro blue tetrazolium (NBT) and 5-bromo-4-chloro-3-indolyl-phosphate (BCIP) staining for single labeling, or NBT/BCIP followed by iodonitrotetrazolium (INT) and BCIP staining for double labeling. For sagittal sections, larvae were embedded in OCT (Sakura) and sectioned on a Leica cryostat. All in situ data were collected on a Leica DM6000B microscope with a 5× or 20× objective.

Immunofluorescence

For whole-mount immunohistochemistry with rabbit or mouse antibodies, 4-dpf larvae were fixed overnight in 4% paraformaldehyde and stored at –20°C in methanol. Samples were permeabilized by treatment with 10 μg/ml proteinase K, refixed in 4% paraformaldehyde, and blocked in PBS with 0.1% Triton X-100, 10% sheep serum, 1% DMSO, 1% BSA (PBSTrS). For antibody labeling, rabbit anti-Lov or anti-Ron (1:500) (Gamse et al., 2005), rabbit anti-GFP (1:1000, Torrey Pines Biolabs), mouse anti-opsin (1:500) (Adamus et al., 1991) or mouse anti-Zpr1 (1:250, Zebrafish International Resource Center, Eugene, OR) were used. Larvae were incubated overnight in primary antibody diluted in PBSTrS. Primary antibody was detected using goat anti-rabbit or goat anti-mouse secondary antibodies conjugated to the Alexa 568 or Alexa 488 fluorophores (1:350, Molecular Probes).

To simultaneously detect Lov and Ron, chicken anti-Lov polyclonal antibody was generated. A bacterially expressed C-terminal fragment of Lov was generated and purified as described previously (Gamse et al., 2005), injected into hens, and total IgY was isolated from egg yolks (Aves Labs). For Lov/Ron double labeling, larvae were fixed in 100% Prefer fixative (Anatech) overnight and stored in PBS containing 0.1% Tween 20 for up to 2 weeks. Samples were permeabilized, refixed and blocked as above, then incubated overnight with chicken anti-Lov (1:500 dilution of total IgY) and rabbit anti-Ron (1:500) antibodies simultaneously in PBSTrS, and primary antibodies detected with goat anti-chicken:Alexa 568 and goat anti-rabbit:Alexa 488 (1:350, Molecular Probes). All immunofluorescence data were collected on a Zeiss/Perkin Elmer spinning disk confocal microscope with a 40× oil-immersion objective and analyzed with Volocity software (Improvision).

Time-lapse imaging

For time-lapse imaging, wild-type or *fby* mutant embryos carrying the transgene (*foxd3:*GFP)^{fkg3} were either uninjected or injected with a 6 ng/nl solution of *tbx2b* splice MO. Embryos were mounted in a 0.8% solution of low-melting-point agarose containing 0.003% 1-phenyl-2-thiourea (PTU) and anesthetized with 0.04% Tricaine. Images were collected on a Zeiss/Perkin Elmer spinning disk confocal microscope with a 40× oil-immersion objective every 15 minutes from 24-48 hpf and analyzed using Volocity software.

Cell ablation

Ablation of a subset of parapineal cells was performed using Tg(*flh:*GFP)^{c161} or Tg(*foxd3:*GFP)^{fkg3} 31-hpf embryos, mounted dorsal-side-up in 0.8% agarose in 35 mm Petri dishes. Parapineal cells were visualized by GFP fluorescence and ~5 cells were ablated by 5-10 pulses/cell from a 440 nm laser beam (Photonic Instruments) focused through a 40× water-immersion objective mounted on a Leica DM6000B microscope. An equivalent number of cells contralateral to the parapineal were ablated in the controls.

RESULTS

The *from beyond* mutation abolishes habenular asymmetry

We screened 4-dpf larvae to identify ENU-induced mutations that altered expression of the K^+ channel tetramerization domain-related (KCTD) gene *leftover* (*lov*). In the habenulae, *lov* is typically expressed at high levels and in a broader domain on the left (Gamse et al., 2003) (Fig. 1A). The *from beyond* (*fby*) mutation reproducibly caused reduced expression of *lov* in the left habenula (Fig. 1B). In WT larvae, the left habenula is larger and contains more neuropil than the right (Gamse et al., 2003; Concha et al., 2000), whereas in *fby* mutants the size and neuropil content of the left habenula was similar to the right (data not shown). Intercrosses between carriers from the original F2 family revealed that *fby* segregates as a simple mendelian recessive mutation (104/438, 24%).

fby mutant larvae developed with normal overall body morphology, formed swim bladders and fed on schedule, but most larvae died at ~2 weeks of age. Rarely, mutants survived to adulthood (4/101, 4%). A morphological phenotype of reduced otic vesicle size was also detected, with 30% of mutant larvae showing fused otoliths in one or both otic vesicles at 4 dpf, and 100% by 7 dpf (data not shown).

Reduced *lov* expression in the left habenula was associated with other alterations in the usual L-R asymmetric pattern of the habenulae. In WT larvae, a smaller area of the left than of the right habenula expresses the KCTD genes *right on* (*ron*; also known as *kctd12.2* – ZFIN) and *dexter* (*dex*; *kctd8* – ZFIN) (Gamse et al., 2005) (Fig. 1C,E). By contrast, the left habenula of *fby* mutant larvae had an expanded region of *ron*- and *dex*-expressing cells similar to the right habenula (Fig. 1D,F).

In addition to asymmetric gene expression, the left and right habenulae differ in their axonal projections to the IPN (Kuan et al., 2007b; Gamse et al., 2005; Aizawa et al., 2005). In WT larvae, Lov^+ axons project to the dorsal and ventral regions of the IPN, whereas Ron^+ axons project to the ventral IPN only (Gamse et al., 2005) (Fig. 1G,I-K). In *fby* mutant larvae, the dorsal/ventral (D/V) pattern of L-R habenula projections was altered. Fewer Lov^+ axons projected dorsally and more projected ventrally (Fig. 1H,L), and an increased number of Ron^+ axons were detected ventrally (Fig. 1M,N). These data are consistent with left habenular efferents adopting a projection pattern characteristic of the right habenula.

The abnormal laterality in the brains of *fby* mutants prompted an examination of asymmetric Nodal signaling, a key early determinant of L-R axis formation (Shen, 2007). In WT embryos, two Nodal genes, *southpaw* (*spaw*) and *cyclops* (*cyc*; also known as *ndr2* – ZFIN), are expressed in the zebrafish left lateral plate mesoderm (LPM), as are the Nodal-induced genes *lefty1* (*lft1*) and *pitx2* (Sampath et al., 1998; Rebagliati et al., 1998b; Rebagliati et al., 1998a; Long et al., 2003; Liang et al., 2000; Concha et al., 2000; Bisgrove et al., 2000) (see Fig. 2A,B). *cyc*, *lft1* and *pitx2* were also expressed in the left side of the epithalamus (Fig. 2C-E). In *fby* mutants, expression of *spaw*, *cyc*, *lft1* and *pitx2* was indistinguishable from that in WT siblings in both the left LPM and left epithalamus (Fig. 2F-J). The right-sided position of the pancreas and rightward looping of the heart tube, which are influenced by Nodal signaling in the left LPM (Yan et al., 1999), were also unaffected in *fby* mutants (data not shown).

fby mutants have fewer and mispositioned parapineal cells

Previous studies have shown that the left-sided parapineal organ is required for the asymmetric identity of the habenulae, and therefore for L-R habenular neurons to adopt D/V differences in their projection to the IPN (Gamse et al., 2003; Gamse et al., 2005; Concha et al., 2003; Aizawa et al., 2005). To determine if the altered laterality of the habenulae in *fby* mutants was due to disrupted development of the parapineal, we examined pineal complex formation.

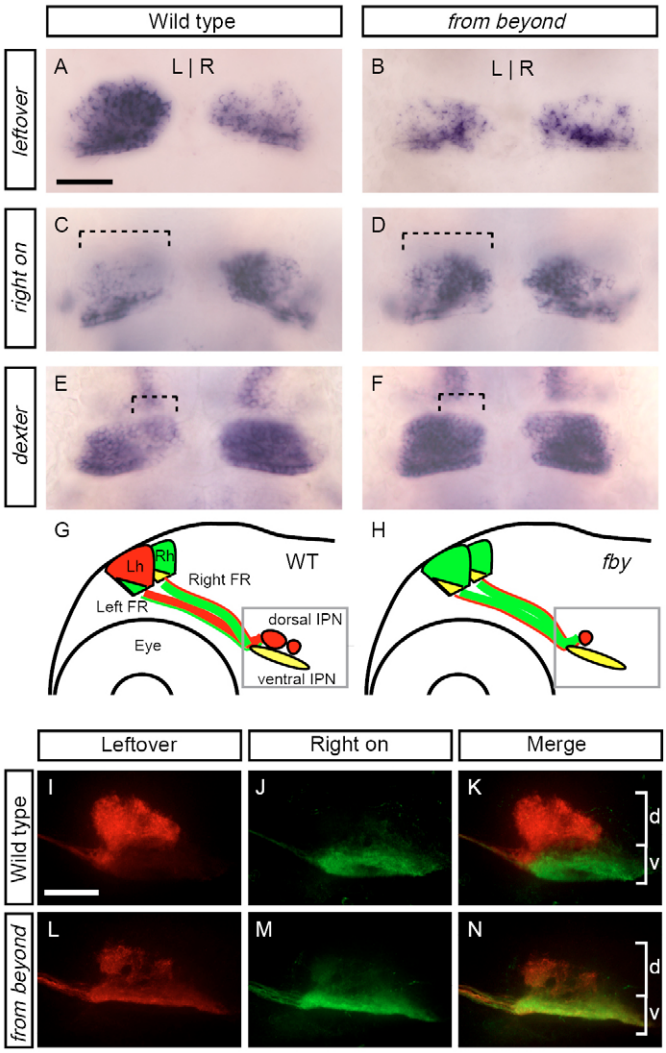

Fig. 1. The left and right habenulae develop more symmetrically in *from beyond* (*fby*) mutants. (**A-F**) Dorsal views of the epithalamus of 4-dpf zebrafish larvae. (A) In wild-type (WT) larvae, the KCTD gene *leftover* (*lov*) was expressed in more cells of the left (L) than of the right (R) habenula. (B) In *fby* mutant larvae, the number of *lov*-expressing cells in the left habenula was reduced relative to WT. In WT (C,E), the *lov*-related *right on* (*ron*) and *dexter* (*dex*) genes were expressed in more cells of the right than of the left habenula, but in *fby* mutants (D,F), *ron* and *dex* habenular expression appeared symmetrical. Brackets indicate the regions where expression was expanded in the mutants. (**G-N**) Lateral views of the brain of 4-dpf larvae. Diagrams depicting projections from the habenular nuclei (Lh and Rh) via the fasciculi retroflexus (FR) to the interpeduncular nucleus (IPN) in WT (G) and *fby* mutant (H) larvae at 4 dpf. Red and green areas indicate Lov and Ron immunoreactive neurons, respectively; yellow indicates colocalization of Lov and Ron; gray boxes indicate the area of the brain imaged in I-N. In WT, (I) an antibody against Lov labeled habenular efferents that terminated in both the dorsal and ventral IPN, whereas (J) an antibody against Ron labeled axons terminating in the ventral IPN. (K) Overlay of I and J. In *fby* mutants, (L) Lov labeling decreased in the dorsal IPN and increased in the ventral IPN, and (M) Ron labeling increased in the ventral IPN. (N) Overlay of L and M. Brackets labeled d and v indicate dorsal and ventral regions of the IPN. Scale bars: 25 μm.

DEVELOPMENT

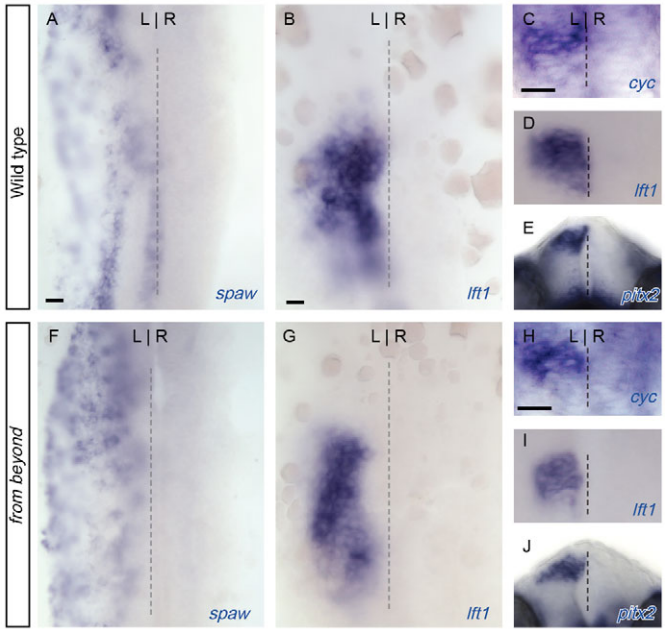

Fig. 2. Asymmetric expression of Nodal pathway components is unaffected by the *fby* mutation. (**A**,**B**,**F**,**G**) The lateral plate mesoderm and (**C-E**,**H-J**) the dorsal diencephalon of 20-hpf zebrafish embryos. All views are dorsal, except for frontal views in E and J. Left-sided expression of the Nodal-related genes *southpaw* (*spaw*; A,F) and *cyclops* (*cyc*; C,H), the Nodal antagonist *lefty1* (*lft1*; B,D,G,I), and of the downstream Nodal effector *pitx2* (E,J) was observed in both WT and *fby* mutant embryos during somitogenesis. Scale bars: 25 μm.

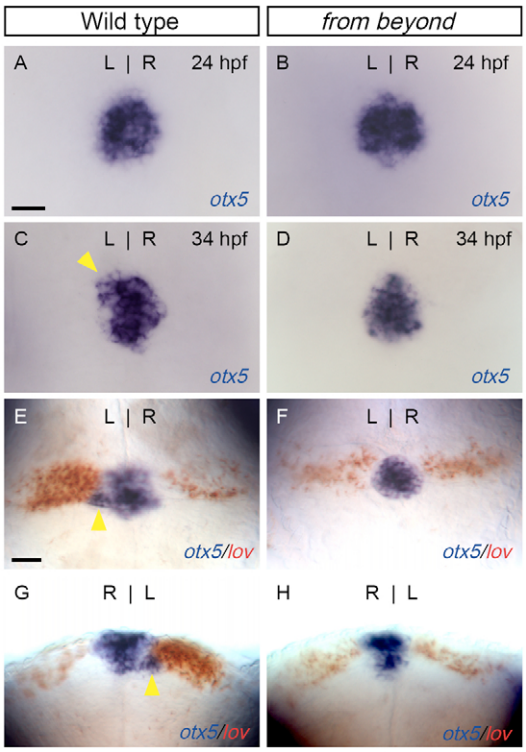

Fig. 3. Disruption of parapineal formation in *fby* mutant zebrafish larvae. (A-F) Dorsal and (G,H) frontal views of the epithalamus of (A,C,E,G) WT and (B,D,F,H) *fby* mutant larvae. (**A**,**B**) At 24 hpf, the pineal complex anlage labeled with *otx5* (blue) appeared similar in WT embryos (A) and *fby* mutants (B). (**C**,**D**) However, by 34 hpf, when a parapineal was apparent in WT embryos (C), no parapineal organ developed in *fby* mutants (D). Arrowhead in C indicates the emerging parapineal organ. (**E**,**G**) By 4 dpf, WT larvae had a left-sided parapineal organ (arrowheads) and more cells expressed *lov* (red) in the left habenula. (**F**,**H**) In *fby* mutant larvae, no left-sided parapineal organ was apparent; rather, *otx5*-expressing cells were found below the pineal organ. The number of *lov*-expressing cells in the left habenula was reduced compared with WT. Scale bars: 25 μm.

The pineal complex adopted an abnormal morphology in *fby* mutants. In 24-hpf WT larvae, the *otx5* gene is expressed throughout the pineal complex anlage (Gamse et al., 2002) (Fig. 3A). By 34 hpf, the *otx5*-expressing parapineal is revealed as a morphologically distinct group of cells emerging from the left anterior border of the pineal complex anlage (Gamse et al., 2002) (Fig. 3C). By 4 dpf, parapineal cells are found in a more posterior and ventral position adjacent to the left habenula (Gamse et al., 2003; Concha et al., 2003) (Fig. 3E,G). In *fby* mutants, the pineal complex anlage appeared similar to WT at 24 hpf (Fig. 3B), but by 34 hpf a distinct parapineal organ was not found (Fig. 3D). At 4 dpf, individual *otx5*-expressing cells were ectopically located below the pineal organ (Fig. 3F,H).

A number of molecular tools allow pineal and parapineal cells to be distinguished in WT larvae. The *growth factor independent 1* (*gfi1*) gene is selectively expressed at 48 hpf in a tight cluster of parapineal cells on the left side of the brain (10±1 cells, n=23) (Dufourcq et al., 2004) (see Fig. 4A,C and Table 1) and are never detected in the pineal. We also examined pineal-specific markers, in the context of the transgenic line Tg(*foxd3*:GFP)^{fkg17} that labels both pineal and parapineal cells with GFP (Gilmour et al., 2002; Concha et al., 2003) (see Fig. S1 in the supplementary material). The entire pineal complex of WT larvae consisted of 60±10 GFP-positive cells (n=13, Table 1). Red-green cone cells labeled by the Zpr1 antibody were found in the pineal but were absent from the parapineal (Fig. 4E). Almost half of the GFP-positive pineal cells were identified in confocal sections as red-green cone cells (44%, n=13, Table 1). Rod cells in the dorsal midline of the pineal organ were labeled by the anti-rhodopsin antibody (Concha et al., 2000). Parapineal cells were negative for rhodopsin expression (Fig. 4G,I, Table 1).

In *fby* mutants, some ectopic cells located ventral to the pineal organ were labeled by *gfi1* at 4 dpf (Fig. 4B). However, there were far fewer *gfi1*-expressing cells in mutants than in WT larvae (Table 1), and these were scattered near the midline of the brain, rather than tightly clustered on the left as in WT (Fig. 4D). Some of the ectopic cells in *fby* mutants sent out projections reminiscent of WT parapineal axonal projections to the left habenula (Fig. 4, compare I with J). In mutants, projections from the ectopic cells did not appear to extend to either habenula, as assessed by GFP expression (Fig. 4J and see Fig. S1 in the supplementary material). Other ectopically positioned cells expressed the pineal cone-cell marker Zpr1, but not rhodopsin (Fig. 4F,H,J). These data indicate that the ectopic cell population consisted of a mixture of pineal and parapineal cells. The few parapineal cells that did develop in *fby* mutants failed to organize into a coherent structure.

Migration of a group of cells, such as the lateral line primordium, requires polarization of the cell cluster (reviewed by Ghysen and Dambly-Chaudiere, 2007). The failure of parapineal migration in *fby* mutants could therefore be a secondary consequence of specifying too few parapineal cells to form a polarized group. To test whether parapineal migration and cohesion depend on cell number, ~5 cells

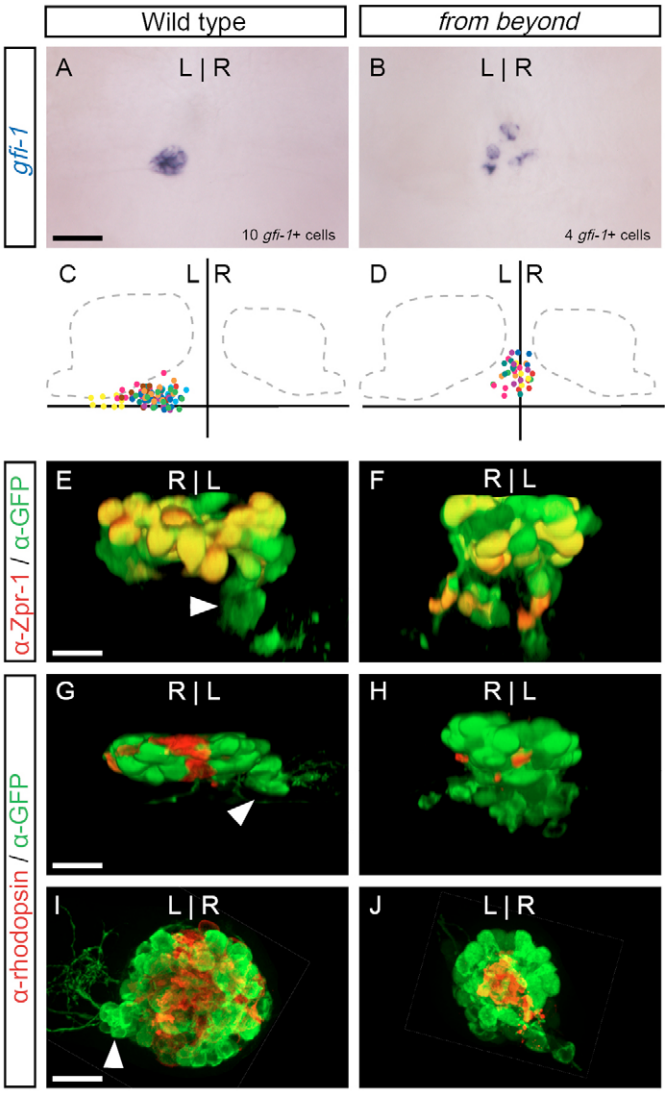

Fig. 4. Fewer and misplaced parapineal cells in *fby* mutants. (A-D,I,J) Dorsal and (E-H) frontal views of 4-dpf zebrafish larvae. (**A**) In the epithalamus, expression of *gfi1* was exclusive to the parapineal cells of WT larvae at 4 dpf, which formed a compact organ. (**B**) In *fby* mutants, fewer *gfi1*-expressing cells developed than in WT, and they were found as individual cells in the middle of the brain. (**C**,**D**) The position of *gfi1*-expressing cells from ten individual WT (C) or *fby* (D) larvae as represented by different colored dots for each sample. The vertical axis divides the left and right sides of the brain, and the horizontal axis is the posterior border of the habenular nuclei. (**E**) Double immunofluorescent labeling of a WT larva with *foxd3:gfp* (green) and the antibody Zpr1 (red). Zpr1 labels red-green double cone cells, which were almost exclusively found in the pineal but not the parapineal (arrowhead). (**F**) In *fby* mutants, Zpr1 labeled cells were found throughout the pineal complex, including cells ventral to the pineal organ. (**G-J**) Double labeling with *foxd3:gfp* (green) and anti-rhodopsin antibody (red). Rhodopsin-expressing cells were near the dorsal midline of the pineal organ in WT (G,I) and (H,J) *fby* mutant larvae. Scale bars: 25 μm.

were ablated at 31 hpf, prior to their movement away from the pineal complex anlage, leaving a number of cells comparable to *fby* mutants (Fig. 5A-F). The placement of the remaining parapineal cells was assayed at 55 hpf, when they have moved leftward, as well as

Table 1. Number of labeled cells present in the pineal complex of *fby* mutants

Gene/protein (cell types labeled)	Genotype	Number of cells*	N
GFP in Tg(*foxd3:gfp*)	WT	60±10	13
(pineal and parapineal cells except rod cells)	*fby*	61±17	12
Zpr1 antibody	WT	21±6	13
(red-green double cone cells)	*fby*	24±6	12
Anti-rhodopsin antibody	WT	41±2	4
(rod cells)	*fby*	37±2	6
gfi1	WT	10±1	23
(parapineal cells)	*fby*	3±2†	23

*Average number of cells labeled per larvae at 4 dpf, plus or minus one s.d.
†Significantly different from WT and *flh* by two-tailed *t*-test, $P<0.01$.
N, number of samples examined.

posteriorly and ventrally, and begin to express *gfi1*. We found that the remaining parapineal cells formed a coherent and correctly positioned, albeit smaller, parapineal organ, similar to controls (Fig. 5G-L).

The *fby* mutation introduces a premature stop codon in the *tbx2b* coding sequence

The *fby* mutation was mapped to a region of chromosome 15, approximately 100 kb telomeric to the SSLP marker z22430 (Fig. 6A). Examination of the zebrafish genome sequence (Hubbard et al., 2007) revealed two genes, *tbx2b* and *tbx4*, in this region. The *tbx2b* gene was a likely candidate based on previous reports of expression in the pineal anlage (Ruvinsky et al., 2000; Dheen et al., 1999) and the observation that antisense morpholino (MO)-treated embryos developed abnormal otic vesicles similar to those seen in *fby* mutants (Gross and Dowling, 2005). Sequencing of *tbx2b* cDNA from *fby* mutants at 4 dpf revealed a T-to-A transversion introducing a premature stop codon (Fig. 6B). This lesion lies within the T-box sequence and is predicted to prevent translation of 9 of the 20 DNA-contacting residues (Sinha et al., 2000). Two different MOs that blocked either *tbx2b* translation or removal of the third intron (Gross and Dowling, 2005) effectively phenocopied the *fby* mutation (Fig. 6C,D). Microinjection of *tbx2b* MOs into *fby* mutants did not cause a further reduction in the number of *gfi1*-expressing cells (data not shown), supporting the premise that the *fby* mutation eliminates *tbx2b* function.

tbx2b is expressed early in the pineal complex anlage

Expression of *tbx2b* in the cells that give rise to the medially located pineal complex anlage was present at the six-somite stage, in two clusters of cells at each lateral edge of the neural plate (Fig. 7A). By the ten-somite stage, when the lateral edges of the neural plate meet to form the neural rod, a single dorsal midline domain of *tbx2b* expression was detected (Fig. 7B) (Ruvinsky et al., 2000). At 24 hpf, expression of *tbx2b* was found in many cells of the pineal complex anlage, and was most intense in the midline (Ruvinsky et al., 2000; Dheen et al., 1999; Cau and Wilson, 2003) (Fig. 7C). At 4 dpf, *tbx2b* expression was maintained in the parapineal organ and the pineal stalk (Fig. 7D). In *fby* mutants, *tbx2b* RNA expression was still detected in the pineal complex anlage at a similar level to that in WT (Fig. 7E,F), indicating that the *fby* mutation did not cause nonsense-mediated decay.

The *tbx2b* expression pattern resembled that of *flh*, a homeobox transcription factor also expressed in the pineal complex anlage (Masai et al., 1997), although the two expression patterns did not completely overlap. During somitogenesis, many *flh*-positive cells

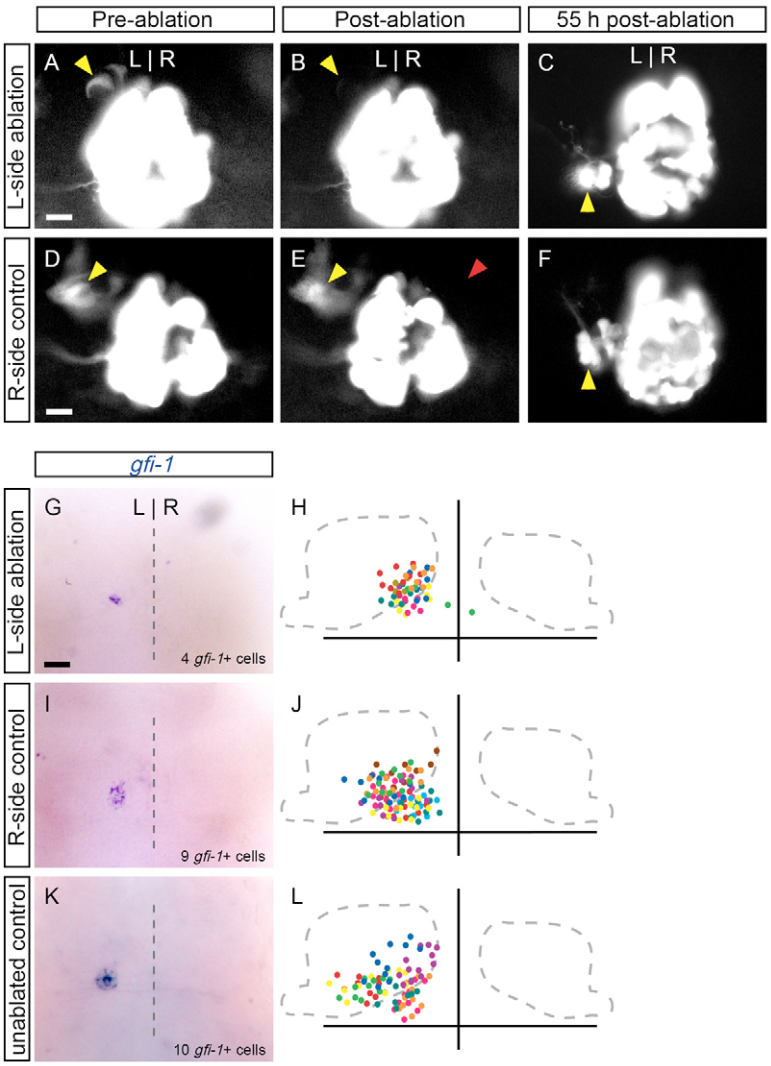

Fig. 5. Reduced numbers of parapineal cells are able to migrate to the left side of the brain. Dorsal views of the epithalamus in (**A**,**B**,**D**,**E**) 31-hpf zebrafish embryos or (**C**,**F**,**G-L**) 55-hpf larvae. Expression of *foxd3:gfp* labels parapineal precursor cells (A, yellow arrowhead), which are subsequently ablated with laser pulses (B). The remaining parapineal cells (average of 5±2 cells, *n*=18) migrate to the left side of the brain, as revealed by *foxd3:gfp* (C) and *gfi1* (G) expression. In H, the position of *gfi1*-expressing cells in ten larvae are overlaid, with different colors representing individual samples. (D-F) As a control, cells contralateral to the parapineal precurors were ablated (red arrowhead). The number of parapineal cells (10±1, *n*=8) and their migration in these controls (I,J) were identical to those in unablated controls (K,L; 10±2 cells, *n*=10). Scale bars: 25 μm.

expressed *tbx2b* (Fig. 7G). However, some medial cells of the pineal complex anlage expressed *tbx2b* only (Fig. 7H). By 24 hpf, the pineal complex anlage expressed both *flh* and *tbx2b*, except at its most lateral edges, where only *flh* expression was detected (Fig. 7I,J).

Previous reports indicated that during neural plate formation in zebrafish, *tbx2b* expression is regulated by the Wnt receptor *frizzled 7a* (*fzd7a*) (Fong et al., 2005), and that in the developing mouse hindbrain, *Tbx2* regulates expression of Wnt planar cell polarity (PCP) genes including *Fzd7* (Song et al., 2006). However, we find that disrupting the Wnt PCP signaling pathway, by mutation of the proteoglycan *knypek* (*glypican*) (Topczewski et al., 2001) or *van gogh-like 2* (*strabismus*; also known as *trilobite* in zebrafish) (Jessen et al., 2002), has no effect on *tbx2b* expression, parapineal specification or migration (see Fig. S2A-I in the supplementary material). In addition, neither *fzd7a* nor other PCP genes (*wnt11*, *wnt5*, *fzd7b*, *trilobite*) are expressed in the epithalamus (see Fig. S2J-Q in the supplementary material; data not shown).

Migration of parapineal cells is disrupted in *fby* mutants

In *fby*/*tbx2b* mutants, the absence of a distinct left-sided parapineal organ and the development of parapineal cells in an ectopic ventral location suggested that parapineal cells failed to move to the left side of the brain. Although studies have inferred that parapineal precursors migrate out from the anlage to the left side of the brain (Gamse et al., 2003; Concha et al., 2003), these cellular movements have not been directly documented in live embryos. We performed time-lapse analysis using *foxd3:gfp* transgenic embryos, recording cell locations between 24 and 48 hpf (see Movie 1 in the supplementary material). One or two highly protrusive cells extending multiple short and wide filipodia were detected at the anterior left edge of the pineal complex anlage at 31 hpf (Fig. 8A). Over the next 8 hours, these cells migrated in a leftward and slightly caudal direction (Fig. 8D,G). They were very closely followed by more cells that originated from the same anterior left region of the pineal complex anlage (Fig. 8J). By 48 hpf, the cells stopped moving, they coalesced into a tightly packed cluster and extended highly dynamic, thin processes (Fig. 8M,P).

In contrast to the robust migration of parapineal cells to the left side of the brain, leftward migrating cells were not observed in *tbx2b* MO-treated or *fby* homozygous mutant embryos (see Movies 2, 3 in the supplementary material). At 33 hpf, one or two highly protrusive cells were seen at the anterior end of the pineal complex anlage (Fig. 8B,C). They were joined by an additional two or three highly protrusive cells over the next 9 hours (Fig. 8E,F,H,I,K,L). However, these cells did not migrate to the left of the pineal, but remained close to the midline near the anterior end of the pineal complex anlage. Although in an ectopic location, these cells still extended long thin processes by 48 hours (Fig.

DEVELOPMENT

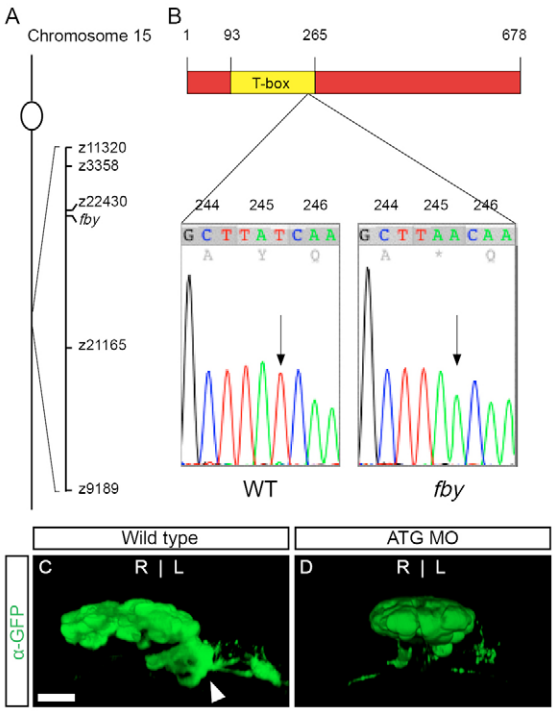

Fig. 6. The *fby* mutation is a premature stop codon in the *tbx2b* gene. (**A**) Diagram of zebrafish chromosome 15, showing the location of the *fby* mutation relative to nearby SSLP markers. (**B**) In *fby*^{c144} mutants, the third position of codon 245 in the *tbx2b* gene was transverted from T to A, generating a stop codon within the T-box sequence. (**C**,**D**) Frontal views of 4-dpf larvae. Compared with uninjected *foxd3:gfp* controls (C), injection of an antisense morpholino against the start codon of *tbx2b* (ATG MO) resulted in a similar phenotype to the *fby* mutation (D). Scale bar: 25 μm.

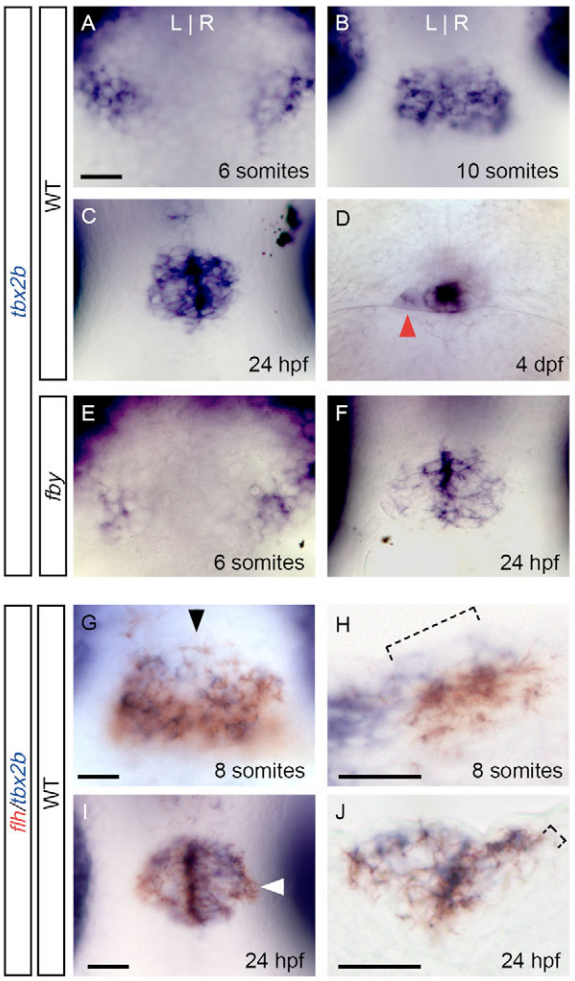

Fig. 7. *tbx2b* expression in the pineal complex. (A-G,I) Dorsal views of zebrafish embryos or larvae at the indicated stages of development. (H) A sagittal section at the level of the arrowhead in G. (J) A transverse section at the level of the arrowhead in I. (**A**) Expression of *tbx2b* in the future epithalamus began at six somites, in two groups of cells at the lateral borders of the neural plate. (**B**,**C**) Following neural tube closure, a single *tbx2b*-expressing domain was detected at ten somites (B) and 24 hpf (C). (**D**) At 4 dpf, expression was maintained in the parapineal (arrowhead) and in the pineal stalk. (**E**,**F**) Expression of *tbx2b* was unchanged in *fby* mutants at ten somites (E) and 24 hpf (F). (**G**,**H**) Many *tbx2b*-expressing cells (blue) also expressed *flh* (red) in the future epithalamus at eight somites (G), although some *tbx2b*$^{+}$ *flh*$^{-}$ cells were detected medially and dorsally (H, bracket). (**I**,**J**) By 24 hpf, *tbx2b* and *flh* were co-expressed in much of the pineal complex anlage (I), although expression of *flh* extended slightly more laterally and ventrally (J, bracket) than *tbx2b*. Scale bars: 25 μm.

8N,O,Q,R). The time-lapse analyses indicated that *tbx2b* is required for the leftward migration of parapineal cells and their morphogenesis into a coherent cluster.

DISCUSSION

In this study, we examined the specification and migration of cells that form the parapineal organ using the *fby* mutation, which disrupts the Tbx2b transcription factor. In *fby* mutants, fewer parapineal cells develop, and these cells fail to migrate to the left side of the brain to coalesce into the parapineal organ. Our findings have therefore identified a genetic regulator of a distinct subpopulation of cells in the pineal complex anlage that is important for their specification and migration.

Expression of *tbx2b* in the pineal complex specifies parapineal cells

The *tbx2b* gene is expressed in many cells of the pineal complex anlage, but only a dozen cells contribute to the parapineal organ. How does a widely expressed transcription factor play a role in the development of a limited number of parapineal cells? One likely model is that different cell types in the pineal complex anlage are specified by different repertoires of transcription factors that interact with *tbx2b*. Modulation of enhancer-binding activity by interaction with other transcription factors (particularly Lim, Gata and homeodomain proteins) is a common feature of Tbx family members (Showell et al., 2004; Naiche et al., 2005). The *tbx2b* gene is co-expressed with the homeobox gene *flh* in most of the pineal complex anlage at eight somites. However, a small symmetric domain in the anterior medial region of the anlage expresses *tbx2b* but not *flh*. We propose that cells from this anterior medial domain will be specified as parapineal, whereas cells expressing both *flh* and *tbx2b* will generate the pineal organ. This model predicts that the *fby* mutation causes parapineal precursors to be respecified to a pineal fate. In support of this model, we find that in addition to reduced numbers of *gfi1*-expressing parapineal cells, red-green cone cells typically restricted to the pineal are instead situated in an ectopic position ventral to the pineal organ.

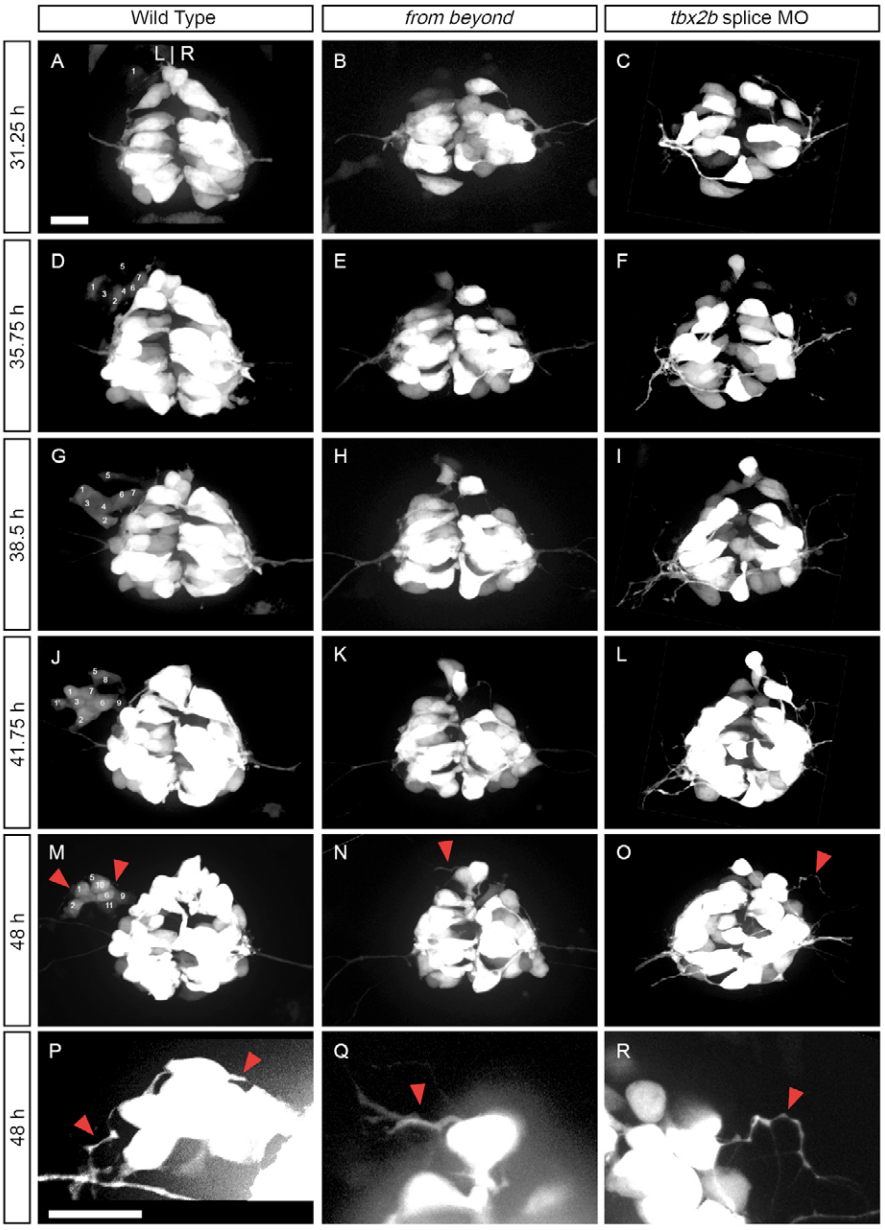

Fig. 8. Parapineal cells do not migrate to the left side of the brain in *fby* mutants. Dorsal views of *foxd3:gfp* expression in live (**A**,**D**,**G**,**J**,**M**,**P**) WT, (**B**,**E**,**H**,**K**,**N**,**Q**) *fby* mutant or (**C**,**F**,**I**,**L**,**O**,**R**) *tbx2b* splice morpholino-treated embryos. The data are snapshots of time-lapse confocal movies imaged from 31 to 48 hpf. P,Q,R are magnified and contrast-enhanced regions of the anterior pineal complex from M,N,O, respectively. In WT embryos, GFP-labeled cells emerged from the anterior left end of the pineal complex as a chain of cells between 31 and 39 hpf. Cells are numbered in the order of their appearance. Cell 1 divided from 39.75 to 40.25, and its daughter is labeled 1′. Note that some parapineal cells (e.g. #3, 4, 7, 8) become hidden by overlying cells. Between 39 and 48 hpf, the parapineal cells compacted together, and extended long thin projections (red arrowhead). By contrast, *fby* mutants and *tbx2b* morpholino-treated embryos had no GFP-labeled cells migrating to the left, but cells at the anterior end of the pineal complex still extended long thin projections. Scale bar: 25 μm.

The absence of a *tbx2b*-exclusive domain in the pineal complex anlage of *fby* mutants affects parapineal specification; however, a few cells still adopt parapineal identity as assessed by *gfi1* expression. The action of *tbx2b* in combination with additional transcription factors during parapineal and pineal specification will be directly tested by conditional misexpression in the epithalamus using tissue-specific promoters.

A trivial explanation for the formation of a few *gfi1*-expressing cells in *fby* mutants is that the mutation is hypomorphic; however, the c144 ENU lesion produces a premature stop codon that is predicted to abolish Tbx2b binding to DNA. Moreover, depletion of *tbx2b* in WT or *fby* mutant embryos by two highly effective MOs phenocopied all aspects of the *fby* mutation, but did not eliminate *gfi1*-expressing cells completely. It is unlikely that a second zebrafish Tbx gene partially compensates for the loss of *tbx2b*, because the closest relatives of *tbx2b* (*tbx2a*, *tbx3*, *tbx4* and *tbx5*) do not appear to be expressed in the pineal primordium (Ruvinsky et al., 2000; Dheen et al., 1999).

tbx2b specifies parapineal cells without affecting Nodal signaling

In addition to expression in the pineal complex, *tbx2b* is expressed in the chordoneural hinge (CNH), a structure in the embryonic tailbud (Ruvinsky et al., 2000; Dheen et al., 1999). Expression of the Nodal gene *southpaw* in the CNH is required for its subsequent asymmetric expression in the left LPM, where it regulates left-sided expression of another Nodal gene, *cyc*, in the LPM and epithalamus (Gourronc et al., 2007). Loss of *spaw* activity results in the absence of *cyc* expression in the left epithalamus (Long et al., 2003) and in L-R randomization of parapineal location (Gamse et al., 2005). However, *fby* mutant embryos develop with normal left-sided expression of Nodal genes, indicating that *tbx2b* activity in the CNH is not required for initiation of asymmetric *spaw* expression. This suggests that *tbx2b* acts in the pineal complex anlage to regulate specification of the parapineal organ in a pathway that is independent of Nodal signaling.

DEVELOPMENT

Parapineal cells require *tbx2b* activity to migrate away from the pineal complex anlage

In WT embryos, migration of parapineal precursor cells from the pineal complex anlage begins with the emergence of a single cell from the anterior left region, followed by other closely apposed cells. This sequence suggests a leader-follower mechanism for directional migration, in which cells at the leading edge coordinate the behavior of the group. Such cellular behavior has been best described in zebrafish for the migration of the lateral line primordium, where leader cells expressing *cxcr4b* at the anterior end of the primordium organize the migration of the rest of the cells (Haas and Gilmour, 2006). The first cells to emerge from the pineal complex anlage may be leader cells that direct the left-sided movement of the parapineal organ. In *fby* mutants, a reduced number of cells develop with parapineal characteristics, including *gfi1* expression and anteriorward axonal projections, and they do not migrate to the left side of the epithalamus; rather, at 48 hpf they are found in the midline, at the anterior edge of the pineal complex. The failure of parapineal cells to migrate in *fby* mutants could be due to the reduced number of parapineal precursor cells that are specified, the inability of mutant cells to move, or a loss of leader cell function. We believe that the latter hypothesis is correct. First, reducing the total number of parapineal precursor cells by laser ablation to a number similar to that of the scattered cells in the *fby* mutant, still allows a cohesive organ to form on the left side of the brain. Second, *fby* mutant parapineal cells still move posteriorly and ventrally, and thus are not immobile. Therefore, we speculate that *tbx2b* is required for the specification or maintenance of leader cells. Testing this hypothesis will require the development of methods to identify the leader cells and specifically destroy them as they emerge from the pineal complex.

One mechanism invoked to mediate *tbx2b* regulation of migration is the Wnt-PCP pathway. Although *tbx2b* plays a role in PCP in other contexts (Fong et al., 2005; Song et al., 2006), we find no role for PCP in parapineal migration.

Delayed parapineal migration away from the midline until after 48 hpf has been observed in *masterblind* (*mbl*; also known as *axin1*) and RNA-rescued *one-eyed pinhead* (R*oep*) mutants in a significant percentage of larvae (Gamse et al., 2002; Carl et al., 2007). However, by 96 hpf, the parapineal cells of *mbl* and R*oep* mutants have achieved their correct left-sided position, whereas the parapineal cells of *fby* mutants remain scattered close to the midline. The data suggest that *mbl* and *oep* regulate the timing or speed of migration, but are not required for leader cell formation.

An evolutionarily conserved role for Tbx genes in parapineal formation?

Fish, frog, lizard and bird embryos all develop a pineal and a pineal accessory organ (although in birds the parapineal does not persist in the adult), whereas mammals seem to form only the pineal gland (Hill, 1892; Butler and Hodos, 1996; Braitenberg and Kemali, 1970; Borg et al., 1983). The development of a pineal complex that includes both a pineal and an accessory organ is phylogenetically correlated with the expression of Tbx homeobox genes in the pineal complex anlage. Such expression is observed for *tbx2b* in zebrafish (Ruvinsky et al., 2000; Dheen et al., 1999) (this study), and for the closely related *Tbx3* gene in chick (Gibson-Brown et al., 1998) and *Xenopus* (Takabatake et al., 2000). However, in the mouse, neither *Tbx2* nor *Tbx3* is expressed in the developing diencephalon (Chapman et al., 1996). We propose that the pineal accessory organ of non-mammalian vertebrates is specified by Tbx2/3 function.

In lizards and frogs, the pineal accessory organ (known as the parietal eye or frontal organ, respectively) is photoreceptive, expresses certain opsin family members and is thought to transmit diurnal information (Engbretson et al., 1981; Eldred et al., 1980; Su et al., 2006; Blackshaw and Snyder, 1997). In mammals, which do not receive direct light input to the pineal, the major source of diurnal information is stimulation of the melanopsin-expressing retinal ganglion cells (Hattar et al., 2002). The acquisition of photic input to the pineal via the eyes in mammals rendered a photoreceptive pineal accessory organ unnecessary. Loss of *Tbx2/3* expression in the pineal complex anlage might be the mechanism that prevents formation of a pineal accessory organ in mammals, by altered specification and disrupted migration of precursors. How a transcription factor regulates the number and behavior of parapineal cells will be revealed by identification of its downstream target genes.

We thank Jeff Gross and John Dowling for *tbx2b* morpholino reagents; Paul Hargrave for the rhodopsin antibody; Lila Solnica-Krezel for *knypek* mutants and PCP gene clones; Jason Jesson for *trilobite* mutants; Chris Wright and Bruce Appel for valuable discussions; and Lijun Bian, Erin Booton and Lea Fortuno for technical help. Support was provided by a zebrafish initiative funded by the Vanderbilt University Academic Venture Capital Fund and a grant from the Whitehall Foundation to J.T.G., and a N.I.H. grant (HD042215) to M.E.H.

Supplementary material

Supplementary material for this article is available at
http://dev.biologists.org/cgi/content/full/135/9/1693/DC1

References

Adamus, G., Zam, Z. S., Arendt, A., Palczewski, K., McDowell, J. H. and Hargrave, P. A. (1991). Anti-rhodopsin monoclonal antibodies of defined specificity: characterization and application. *Vision Res.* **31**, 17-31.

Aizawa, H., Bianco, I. H., Hamaoka, T., Miyashita, T., Uemura, O., Concha, M. L., Russell, C., Wilson, S. W. and Okamoto, H. (2005). Laterotopic representation of left-right information onto the dorso-ventral axis of a zebrafish midbrain target nucleus. *Curr. Biol.* **15**, 238-243.

Bahary, N., Davidson, A., Ransom, D., Shepard, J., Stern, H., Trede, N., Zhou, Y., Barut, B. and Zon, L. I. (2004). The Zon laboratory guide to positional cloning in zebrafish. *Methods Cell Biol.* **77**, 305-329.

Bisgrove, B. W., Essner, J. J. and Yost, H. J. (2000). Multiple pathways in the midline regulate concordant brain, heart and gut left-right asymmetry. *Development* **127**, 3567-3579.

Blackshaw, S. and Snyder, S. H. (1997). Parapinopsin, a novel catfish opsin localized to the parapineal organ, defines a new gene family. *J. Neurosci.* **17**, 8083-8092.

Borg, B., Ekstrom, P. and Van Veen, T. (1983). The parapineal organ of teleosts. *Acta Zoolog.* **64**, 211-218.

Braitenberg, V. and Kemali, M. (1970). Exceptions to bilateral symmetry in the epithalamus of lower vertebrates. *J. Comp. Neurol.***138**, 137-146.

Butler, A. B. and Hodos, W. (1996). *Comparative Vertebrate Neuroanatomy: Evolution and Adaptation*. New York: Wiley-Liss.

Carl, M., Bianco, I. H., Bajoghli, B., Aghaallaei, N., Czerny, T. and Wilson, S. W. (2007). Wnt/Axin1/beta-catenin signaling regulates asymmetric nodal activation, elaboration, and concordance of CNS asymmetries. *Neuron* **55**, 393-405.

Cau, E. and Wilson, S. W. (2003). Ash1a and Neurogenin1 function downstream of Floating head to regulate epiphysial neurogenesis. *Development* **130**, 2455-2466.

Chapman, D. L., Garvey, N., Hancock, S., Alexiou, M., Agulnik, S. I., Gibson-Brown, J. J., Cebra-Thomas, J., Bollag, R. J., Silver, L. M. and Papaioannou, V. E. (1996). Expression of the T-box family genes, Tbx1-Tbx5, during early mouse development. *Dev. Dyn.* **206**, 379-390.

Concha, M. L., Burdine, R. D., Russell, C., Schier, A. F. and Wilson, S. W. (2000). A nodal signaling pathway regulates the laterality of neuroanatomical asymmetries in the zebrafish forebrain. *Neuron* **28**, 399-409.

Concha, M. L., Russell, C., Regan, J. C., Tawk, M., Sidi, S., Gilmour, D. T., Kapsimali, M., Sumoy, L., Goldstone, K., Amaya, E. et al. (2003). Local tissue interactions across the dorsal midline of the forebrain establish CNS laterality. *Neuron* **39**, 423-438.

Dheen, T., Sleptsova-Friedrich, I., Xu, Y., Clark, M., Lehrach, H., Gong, Z. and Korzh, V. (1999). Zebrafish tbx-c functions during formation of midline structures. *Development* **126**, 2703-2713.

Dufourcq, P., Rastegar, S., Strahle, U. and Blader, P. (2004). Parapineal specific expression of gfi1 in the zebrafish epithalamus. *Gene Expr. Patterns* **4**, 53-57.
Eldred, W. D., Finger, T. E. and Nolte, J. (1980). Central projections of the frontal organ of Rana pipiens, as demonstrated by the anterograde transport of horseradish peroxidase. *Cell Tissue Res.* **211**, 215-222.
El-Messaoudi, S. and Renucci, A. (2001). Expression pattern of the frizzled 7 gene during zebrafish embryonic development. *Mech. Dev.* **102**, 231-234.
Engbretson, G. A., Reiner, A. and Brecha, N. (1981). Habenular asymmetry and the central connections of the parietal eye of the lizard. *J. Comp. Neurol.* **198**, 155-165.
Fong, S. H., Emelyanov, A., Teh, C. and Korzh, V. (2005). Wnt signalling mediated by Tbx2b regulates cell migration during formation of the neural plate. *Development* **132**, 3587-3596.
Gamse, J. T., Shen, Y. C., Thisse, C., Thisse, B., Raymond, P. A., Halpern, M. E. and Liang, J. O. (2002). Otx5 regulates genes that show circadian expression in the zebrafish pineal complex. *Nat. Genet.* **30**, 117-121.
Gamse, J. T., Thisse, C., Thisse, B. and Halpern, M. E. (2003). The parapineal mediates left-right asymmetry in the zebrafish diencephalon. *Development* **130**, 1059-1068.
Gamse, J. T., Kuan, Y. S., Macurak, M., Brosamle, C., Thisse, B., Thisse, C. and Halpern, M. E. (2005). Directional asymmetry of the zebrafish epithalamus guides dorsoventral innervation of the midbrain target. *Development* **132**, 4869-4881.
Ghysen, A. and Dambly-Chaudiere, C. (2007). The lateral line microcosmos. *Genes Dev.* **21**, 2118-2130.
Gibson-Brown, J. J., Agulnik, S. I., Silver, L. M. and Papaioannou, V. E. (1998). Expression of T-box genes Tbx2-Tbx5 during chick organogenesis. *Mech. Dev.* **74**, 165-169.
Gilmour, D. T., Maischein, H. M. and Nusslein-Volhard, C. (2002). Migration and function of a glial subtype in the vertebrate peripheral nervous system. *Neuron* **34**, 577-588.
Gourronc, F., Ahmad, N., Nedza, N., Eggleston, T. and Rebagliati, M. (2007). Nodal activity around Kupffer's vesicle depends on the T-box transcription factors Notail and Spadetail and on Notch signaling. *Dev. Dyn.* **236**, 2131-2146.
Gross, J. M. and Dowling, J. E. (2005). Tbx2b is essential for neuronal differentiation along the dorsal/ventral axis of the zebrafish retina. *Proc. Natl. Acad. Sci. USA* **102**, 4371-4376.
Haas, P. and Gilmour, D. (2006). Chemokine signaling mediates self-organizing tissue migration in the zebrafish lateral line. *Dev. Cell* **10**, 673-680.
Hattar, S., Liao, H. W., Takao, M., Berson, D. M. and Yau, K. W. (2002). Melanopsin-containing retinal ganglion cells: architecture, projections, and intrinsic photosensitivity. *Science* **295**, 1065-1070.
Hill, C. (1892). Development of the epiphysis in Coregonus Albus. *J. Morphol.* **5**, 503-510.
Hubbard, T. J., Aken, B. L., Beal, K., Ballester, B., Caccamo, M., Chen, Y., Clarke, L., Coates, G., Cunningham, F., Cutts, T. et al. (2007). Ensembl 2007. *Nucleic Acids Res.* **35**, D610-D617.
Jessen, J. R., Topczewski, J., Bingham, S., Sepich, D. S., Marlow, F., Chandrasekhar, A. and Solnica-Krezel, L. (2002). Zebrafish trilobite identifies new roles for Strabismus in gastrulation and neuronal movements. *Nat. Cell Biol.* **4**, 610-615.
Kuan, Y. S., Gamse, J. T., Schreiber, A. M. and Halpern, M. E. (2007a). Selective asymmetry in a conserved forebrain to midbrain projection. *J. Exp. Zoolog. B Mol. Dev. Evol.* **308**, 669-678.
Kuan, Y. S., Yu, H. H., Moens, C. B. and Halpern, M. E. (2007b). Neuropilin asymmetry mediates a left-right difference in habenular connectivity. *Development* **134**, 857-865.
Liang, J. O., Etheridge, A., Hantsoo, L., Rubinstein, A. L., Nowak, S. J., Izpisua Belmonte, J. C. and Halpern, M. E. (2000). Asymmetric nodal signaling in the zebrafish diencephalon positions the pineal organ. *Development* **127**, 5101-5112.
Long, S., Ahmad, N. and Rebagliati, M. (2003). The zebrafish nodal-related gene southpaw is required for visceral and diencephalic left-right asymmetry. *Development* **130**, 2303-2316.
Makita, R., Mizuno, T., Koshida, S., Kuroiwa, A. and Takeda, H. (1998). Zebrafish wnt11: pattern and regulation of the expression by the yolk cell and No tail activity. *Mech. Dev.* **71**, 165-176.
Masai, I., Heisenberg, C. P., Barth, K. A., Macdonald, R., Adamek, S. and Wilson, S. W. (1997). floating head and masterblind regulate neuronal patterning in the roof of the forebrain. *Neuron* **18**, 43-57.
Naiche, L. A., Harrelson, Z., Kelly, R. G. and Papaioannou, V. E. (2005). T-Box Genes in Vertebrate Development. *Annu. Rev. Genet.* **39**, 219-239.
Rauch, G.-J., Granato, M. and Haffter, P. (1997). A polymorphic zebrafish line for genetic mapping using SSLPs on high-percentage agarose gels. *Technical Tips Online* **T01208**.
Rebagliati, M. R., Toyama, R., Fricke, C., Haffter, P. and Dawid, I. B. (1998a). Zebrafish nodal-related genes are implicated in axial patterning and establishing left-right asymmetry. *Dev. Biol.* **199**, 261-272.
Rebagliati, M. R., Toyama, R., Haffter, P. and Dawid, I. B. (1998b). cyclops encodes a nodal-related factor involved in midline signaling. *Proc. Natl. Acad. Sci. USA* **95**, 9932-9937.
Ruvinsky, I., Oates, A. C., Silver, L. M. and Ho, R. K. (2000). The evolution of paired appendages in vertebrates: T-box genes in the zebrafish. *Dev. Genes Evol.* **210**, 82-91.
Sampath, K., Rubinstein, A. L., Cheng, A. M., Liang, J. O., Fekany, K., Solnica-Krezel, L., Korzh, V., Halpern, M. E. and Wright, C. V. (1998). Induction of the zebrafish ventral brain and floorplate requires cyclops/nodal signalling. *Nature* **395**, 185-189.
Shen, M. M. (2007). Nodal signaling: developmental roles and regulation. *Development* **134**, 1023-1034.
Showell, C., Binder, O. and Conlon, F. L. (2004). T-box genes in early embryogenesis. *Dev. Dyn.* **229**, 201-218.
Sinha, S., Abraham, S., Gronostajski, R. M. and Campbell, C. E. (2000). Differential DNA binding and transcription modulation by three T-box proteins, T, TBX1 and TBX2. *Gene* **258**, 15-29.
Solnica-Krezel, L., Stemple, D. L., Mountcastle-Shah, E., Rangini, Z., Neuhauss, S. C., Malicki, J., Schier, A. F., Stainier, D. Y., Zwartkruis, F., Abdelilah, S. et al. (1996). Mutations affecting cell fates and cellular rearrangements during gastrulation in zebrafish. *Development* **123**, 67-80.
Song, M. R., Shirasaki, R., Cai, C. L., Ruiz, E. C., Evans, S. M., Lee, S. K. and Pfaff, S. L. (2006). T-Box transcription factor Tbx20 regulates a genetic program for cranial motor neuron cell body migration. *Development* **133**, 4945-4955.
Su, C. Y., Luo, D. G., Terakita, A., Shichida, Y., Liao, H. W., Kazmi, M. A., Sakmar, T. P. and Yau, K. W. (2006). Parietal-eye phototransduction components and their potential evolutionary implications. *Science* **311**, 1617-1621.
Sutherland, R. J. (1982). The dorsal diencephalic conduction system: a review of the anatomy and functions of the habenular complex. *Neurosci. Biobehav. Rev.* **6**, 1-13.
Takabatake, Y., Takabatake, T. and Takeshima, K. (2000). Conserved and divergent expression of T-box genes Tbx2-Tbx5 in Xenopus. *Mech. Dev.* **91**, 433-437.
Talbot, W. S., Trevarrow, B., Halpern, M. E., Melby, A. E., Farr, G., Postlethwait, J. H., Jowett, T., Kimmel, C. B. and Kimelman, D. (1995). A homeobox gene essential for zebrafish notochord development. *Nature* **378**, 150-157.
Thisse, C. and Thisse, B. (1999). Antivin, a novel and divergent member of the TGFbeta superfamily, negatively regulates mesoderm induction. *Development* **126**, 229-240.
Topczewski, J., Sepich, D. S., Myers, D. C., Walker, C., Amores, A., Lele, Z., Hammerschmidt, M., Postlethwait, J. and Solnica-Krezel, L. (2001). The zebrafish glypican knypek controls cell polarity during gastrulation movements of convergent extension. *Dev. Cell* **1**, 251-264.
Tsukui, T., Capdevila, J., Tamura, K., Ruiz-Lozano, P., Rodriguez-Esteban, C., Yonei-Tamura, S., Magallon, J., Chandraratna, R. A., Chien, K., Blumberg, B. et al. (1999). Multiple left-right asymmetry defects in Shh(–/–) mutant mice unveil a convergence of the shh and retinoic acid pathways in the control of Lefty-1. *Proc. Natl. Acad. Sci. USA* **96**, 11376-11381.
Walker, C. (1999). Haploid screens and gamma-ray mutagenesis. In *Methods in Cell Biology*, vol. 60, pp. 43-70. London: Elsevier.
Yan, Y. T., Gritsman, K., Ding, J., Burdine, R. D., Corrales, J. D., Price, S. M., Talbot, W. S., Schier, A. F. and Shen, M. M. (1999). Conserved requirement for EGF-CFC genes in vertebrate left-right axis formation. *Genes Dev.* **13**, 2527-2537.